

Detection of chiral sum frequency generation vibrational spectra of proteins and peptides at interfaces *in situ*

Jie Wang, Xiaoyun Chen, Matthew L. Clarke, and Zhan Chen*

Department of Chemistry, University of Michigan, Ann Arbor, MI 48109

Communicated by Gabor A. Somorjai, University of California, Berkeley, CA, February 15, 2005 (received for review January 10, 2005)

In this work, we demonstrate the feasibility to collect off-electronic resonance chiral sum frequency generation (SFG) vibrational spectra from interfacial proteins and peptides at the solid/liquid interface *in situ*. It is difficult to directly detect a chiral SFG vibrational spectrum from interfacial fibrinogen molecules. By adopting an interference enhancement method, such a chiral SFG vibrational spectrum can be deduced from interference spectra between the normal achiral spectrum and the chiral spectrum. We found that the chiral SFG vibrational spectrum of interfacial fibrinogen was mainly contributed by the β -sheet structure. For a β -sheet peptide tachyplesin I, which may be quite ordered at the solid/liquid interface, chiral SFG vibrational spectra can be collected directly. We believe that these chiral signals are mainly contributed by electric dipole contributions, which can dominate the chiroptical responses of uniaxial systems. For the first time, to our knowledge, this work indicates that the off-electronic resonance SFG technique is sensitive enough to collect chiral SFG vibrational spectra of interfacial proteins and peptides, providing more structural information to elucidate interfacial protein and peptide structures.

chiral vibrational spectroscopy | interfacial proteins and peptides

Understanding chirality is important in biology, chemistry, and medicine. For example, chiral surfaces and interfaces are important in asymmetric chemical synthesis, chiral molecule separation, binding between chiral drugs and proteins, crystal growth, and the adsorption of proteins on biomedical material surfaces. Since the excellent work on chiroptical effects using second-harmonic generation (SHG) was presented by Hicks and coworkers (1–4) and Persoons and coworkers (5–7), extensive research has been performed to investigate such effects in oriented thin films or bulk media by using SHG and sum frequency generation (SFG) spectroscopic techniques (8–38). Many excellent experimental demonstrations and theoretical treatments on this topic have been published in the last decade or so. These studies indicate that more structural information about chiral materials can possibly be deduced by SHG and SFG studies. It has been demonstrated that the nonlinear chiral effect detected by nonlinear optical methods, such as SHG and SFG, can be several orders of magnitude larger than those detected by linear optical methods (refs. 8, 29, and 36 and references therein).

Currently, several general models have been used to interpret the molecular mechanisms of second-order nonlinear chiral spectra (ref. 36 and references therein). Some experimental results can be interpreted by magnetic-dipole contributions and/or interference between electric and magnetic-dipole contributions. For other experiments, the factors mentioned above cannot explain the very strong nonlinear chiral signal observed, and interpretations based on a pure electric-dipole contribution have been proposed. Recently, Shen and coworkers (10, 17) demonstrated that chiral SFG vibrational spectra can be collected from bulk chiral liquids by using the transmission experimental geometry and from a monolayer of molecules at the surface by using electronic resonance enhancement (13). Elec-

tronic resonance enhancement is used to detect chiral SFG vibrational spectra generated from the molecular chirality, because under electronic resonance the asymmetric Raman tensor components will be greatly enhanced by the electronic-vibrational coupling (18). Strong SHG and SFG signals can be observed from chiral molecules; however, Simpson and coworkers (33–37) demonstrated by using SHG that achiral molecules adsorbed on a surface or interface may generate detectable nonlinear optical chiral signals. They concluded that macromolecular orientational effects can dominate the chiroptical responses of uniaxial systems.

Until now, despite the fact that the origins of the nonlinear optical chiral signals can be different (e.g., from the magnetic dipole, interaction between the magnetic dipole and molecular electric dipole, or the macromolecular orientation effect), most SHG or SFG chiral signals studied were electronic resonance signals from small molecules and/or nonresonant signals of large molecules. To our knowledge, no chiral SFG vibrational spectra of adsorbed proteins or peptides at solid/liquid interfaces have been reported yet. Here, we demonstrate that it is feasible to collect chiral SFG vibrational spectra of protein and peptide molecules at the solid/liquid interface. Also, the visible input beam used in the experiment can be far from the electronic resonance; thus, the vibrational-electronic coupling does not need to be considered. Therefore, we believe that such chiral SFG spectra are mainly dominated by contributions from the orientational effect. We show that chiral SFG vibrational spectra are different from “normal” SFG spectra, providing more detailed structural information about protein and peptide molecules at interfaces. To our knowledge, this work is the first to report chiral SFG vibrational spectra from interfacial proteins and peptides experimentally.

Here, we demonstrate that without electronic resonance enhancement, weak chiral SFG vibrational spectra can be collected from an interfacial protein, fibrinogen, by using an interference enhancement technique. The chiral SFG vibrational spectra can be deduced from the interference spectra between weak chiral and strong normal spectra, even when the weak chiral spectra are too weak to be detected directly in the experiment. We also directly collected chiral SFG spectra from an interfacial peptide, tachyplesin I, at the polymer/solution and polymer/water interfaces. The ordered adsorption of the peptide at the interface ensures a very strong chiral SFG vibrational spectrum. Chiral SFG vibrational spectra of both fibrinogen and tachyplesin I were collected from amide I modes. Our studies show clearly that β -sheets contribute stronger chiral signals than other secondary structures. As mentioned, we believe that electric-dipole con-

Abbreviations: PS, polystyrene; SFG, sum frequency generation; SHG, second-harmonic generation; spp, s-polarized SF output, p-polarized visible input beam with a frequency of ω_1 , and p-polarized IR input beam with a frequency of ω_2 ; psp and pps, different polarization combinations similar to spp.

*To whom correspondence should be addressed. E-mail: zhanc@umich.edu.

© 2005 by The National Academy of Sciences of the USA

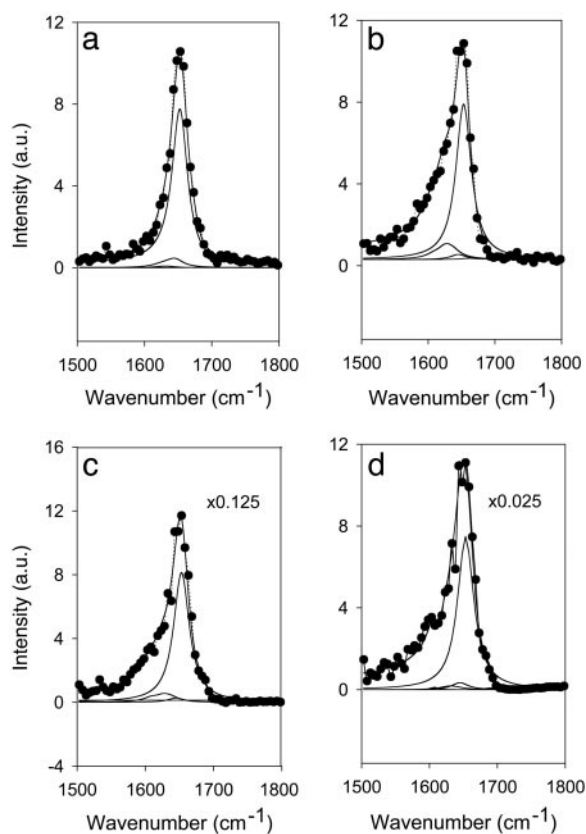


Fig. 1. SFG spectra of the adsorbed fibrinogen layer at the PS/solution interface collected with the following different polarization combinations: $sp - 20^\circ p$ (a), $sp + 20^\circ p$ (b), ssp (c), and ppp (d). Dots are experimental data; lines are fitting results. Fitting components also are shown as lines. a.u., arbitrary units.

Comparing the ppp spectrum with the spp spectrum deduced (Fig. 2), we can see that the two spectra are markedly different. We believe that the spp spectrum we deduced is not the “leaking” spectrum contributed from the ppp spectrum.

The spp spectra with and without the nonresonant background are displayed in Fig. 2. We repeated the experiment several times, and the deduced spp spectra are quite reproducible. From

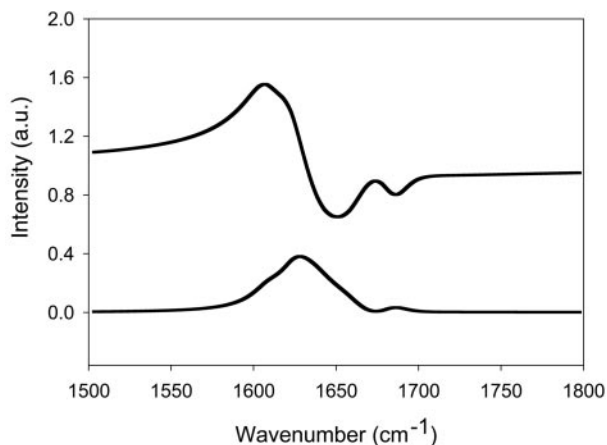


Fig. 2. Deduced chiral SFG vibrational spectra of the adsorbed fibrinogen layer at the PS/solution interface. The upper spectrum has a nonresonant background, and the lower spectrum is a resonant chiral spectrum without the nonresonant background. a.u., arbitrary units.

the spectral fitting, we found that the nonresonant chiral background is quite strong. Its magnitude is comparable to the nonresonant background signals detected in the ssp and ppp spectra. However, compared with the ssp and ppp resonant SFG signals collected from the PS/fibrinogen interface, the resonant spp spectral intensity is much weaker. For SHG studies, off-resonance or nonresonant chiroptical signals at interfaces can be detected. For some cases, the off-resonant SHG chiral signals have comparable strength to the normal SHG signals. The weak chiral SFG vibrational resonant signals deduced here demonstrate the feasibility to detect weak chiral SFG vibrational spectra by using the interference enhancement method. Similar methods can be applied to collect psp and pps spectra. Because the deduced chiral SFG vibrational spectra are very weak, many other factors may play roles to complicate the spectra. The following discussion will further ensure that we indeed collected chiral SFG vibrational spectra.

Because the near-total internal reflection geometry is adopted here to collect SFG spectra, it is necessary for us to discuss the possible effect of the refractive index changes across the resonant peaks. The wavelength-dependent refractive index changes near a resonance peak of the adsorbed protein layer, and the refractive index changes of dilute protein solution due to water bending modes may substantially distort the SFG spectrum (61–65). However, in this experiment, we believe that these refractive index changes would not noticeably affect our SFG spectral features. More details can be found in *Supporting Text*, which is published as supporting information on the PNAS web site.

Our normal ssp and ppp SFG spectra collected from interfacial fibrinogen molecules are dominated by the vibrational peak at $1,650\text{ cm}^{-1}$. We believe that this peak is contributed mainly by the two α -helical coiled-coils connecting the D and E domains in the molecule (57). Detailed data analysis of these SFG spectra can lead to the determination of the conformation of interfacial fibrinogen molecules and should be studied further. The deduced chiral SFG vibrational spectrum is dominated by peaks $\approx 1,630$ and $1,690\text{ cm}^{-1}$, instead of the α -helical $1,650\text{ cm}^{-1}$ peak. According to the peak assignments of secondary structures of proteins, the peaks at $1,630$ and $1,690\text{ cm}^{-1}$ should be contributed from β -sheet structures (66–69). We believe that this characteristic must be due to the fact that β -sheet structures can more easily have ordered twist angles at the interface, thereby generating strong chiral signals for some vibrational modes, as suggested by Simpson and coworkers (35, 36). Our work here clearly indicates that the chiral SFG spectra should provide further structural information about interfacial fibrinogen molecules.

From our above observation, we believe that the β -sheet structures of interfacial proteins should contribute relatively strong chiral SFG vibrational signals. Therefore, if the interfacial proteins or peptides have more ordered β -sheet structures, stronger chiral SFG vibrational spectra may be detected. Perhaps the signal can be strong enough that such chiral spectra can be collected directly without the help of the interference enhancement technique.

We want to point out that the results obtained here are not contradictory to our polarization mapping method published in ref. 56. As we mentioned in that work, if chiral SFG signals are nonzero, a more general method should be used in the polarization mapping treatment. One advantage of the application of the polarization mapping method is that it can test whether detectable SFG chiral signals exist or not (56).

Direct Detection of Strong Chiral Spectra from the Tachyplesin I Peptide at the Solid/Liquid Interface. We used a peptide, tachyplesin I, which has a well characterized structure, as a model system in our following SFG experiments. Tachyplesin I is known to have a β -sheet structure in aqueous environments and at the

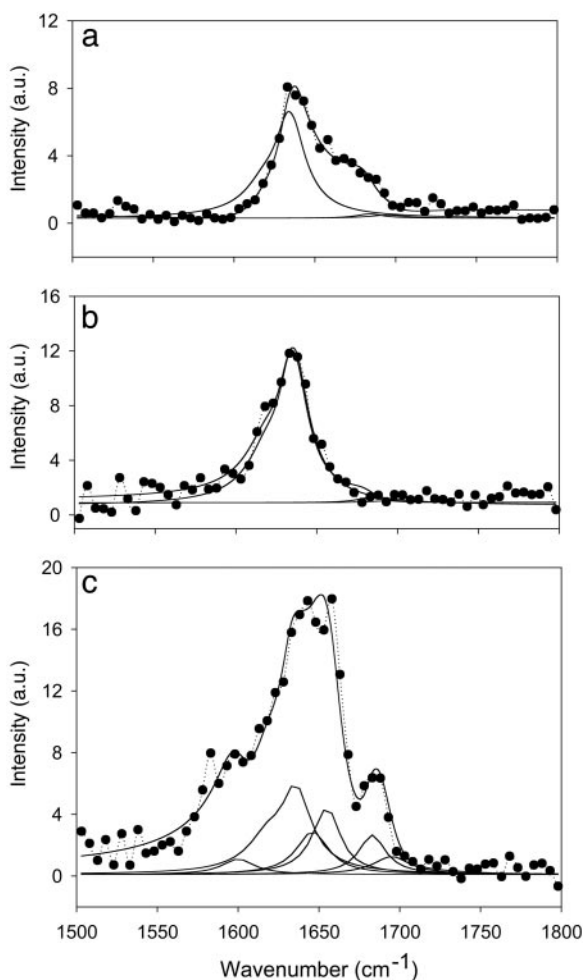


Fig. 3. SFG spectra of adsorbed tachyplesin I at the PS/solution interface with the following different polarization combinations: psp (a), spp (b), and ssp (c). Dots are experimental data; lines are fitting results. Fitting components also are shown as lines. a.u., arbitrary units.

solution/membrane interface (70). The β -sheet structure of tachyplesin I is quite robust because this structure is held together by two disulfide bonds (71). Therefore, we believe that this peptide should still hold a β -sheet structure at the PS/solution interface. We confirmed this finding from both SFG and attenuated total reflection Fourier transform IR spectroscopy studies (71). We believe that the coverage of the β -sheet structure at the PS/tachyplesin I solution interface should be higher than at the PS/fibrinogen solution interface and also have better ordering. If this hypothesis is true, then it is possible to directly collect chiral SFG vibrational spectra. Indeed, in our experiments very strong psp and spp spectra were detected directly from the PS/tachyplesin I solution interface (Fig. 3a and b). The ssp spectrum also was collected for comparison (Fig. 3c). Amazingly, the SFG intensities of spp and psp are comparable with the ssp spectrum but with distinct spectral features. Our spectral fitting results in ref. 71 show that three major peaks can be identified in the ssp spectrum, with the dominating peak at $\approx 1,664 \text{ cm}^{-1}$ and two weaker peaks at $1,645$ and $1,688 \text{ cm}^{-1}$ (71). We believe that the dominating $1,664 \text{ cm}^{-1}$ peak is contributed by amide groups of turns and disordered structures, and the amide peak at $1,688 \text{ cm}^{-1}$ is contributed by the β -sheet structure. The peak at $1,645 \text{ cm}^{-1}$ is a combination peak from the B_2 mode of the antiparallel β -sheet and disordered structures. These three peaks and some lower-wavenumber peaks can fit the SFG

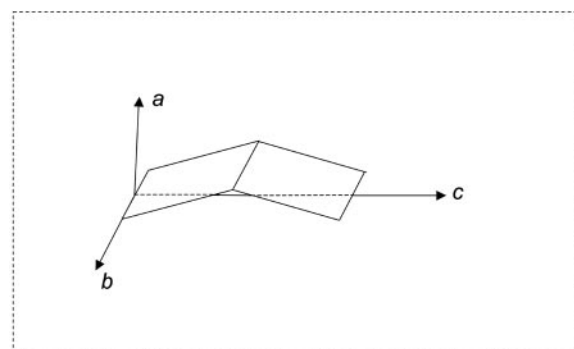


Fig. 4. Molecular coordinate for an antiparallel β -sheet.

spectra quite well. In this work, we attempted to refit the ssp spectrum to accommodate all three SFG active modes of a β -sheet by using a peak at $1,633 \text{ cm}^{-1}$ for the B_2 mode and two peaks at $\approx 1,688 \text{ cm}^{-1}$ for the B_1 and B_3 modes. The best fitting for the ssp spectrum by using such a method contains the following five peaks: $1,633$ (B_2), $1,645$ (disordered structure and β turns), $1,664$ (disordered structure and β turns), $1,685$, and $1,695 \text{ cm}^{-1}$ (B_1/B_3). On the contrary, for the spp and psp spectra, only three major peaks, at $1,633$, $1,685$, and $1,695 \text{ cm}^{-1}$, were observed from the spectral fitting results; the peaks at $1,645$ and $1,664 \text{ cm}^{-1}$ were not detected. This result confirms that β -sheet structure can contribute much stronger chiral SFG vibrational signal and thus dominate the chiral SFG spectra.

Because it is possible for the bulk tachyplesin I molecules in the solution to generate chiral SFG vibrational signals, we performed a further experiment to prove that the chiral SFG spectra were collected from the interfacial molecules. Here, after contacting PS with tachyplesin I solution, we replaced the tachyplesin I solution with water. The same experiment was repeated to collect spp and psp spectra from tachyplesin I at the PS/water interface. Very similar spectra (with similar intensity and spectral features) can be collected from the PS/water interface to those from the PS/solution interface, showing that SFG spectra are contributed from tachyplesin I molecules at the interface rather than in the bulk solution. It is well known that DTT can cleave disulfide bonds (72). We believe that the addition of DTT to the tachyplesin I solution should result in the cleavage of the two disulfide bonds, destroying the β -sheet structure of tachyplesin I. In a previous experiment, we collected the ssp spectrum from the PS/tachyplesin I solution after addition of DTT, and the peak at $1,688 \text{ cm}^{-1}$ disappeared, indicating the lack of β -sheet structure at the interface. However, the dominating peak at $1,664 \text{ cm}^{-1}$ still exists. In the current experiment, no SFG signal can be detected in the spp and psp spectra after the addition of DTT, confirming that β -sheet structures contribute to the strong chiral SFG vibrational spectra.

Further Discussion of Tachyplesin I Results. The repeating unit of an antiparallel β -sheet can be treated as having D_2 symmetry (73). There are four irreducible representations for the D_2 symmetry, A , B_1 , B_2 , and B_3 . Vibrational modes of representation A are only Raman active, whereas the B_1 , B_2 , and B_3 modes are both IR and Raman active. Therefore, theoretically the B_1 , B_2 , and B_3 modes are SFG active. By assuming a molecular coordinate system for an antiparallel β -sheet as shown in Fig. 4, the SFG hyperpolarizability tensor elements (40, 46, 74, 75) can be written as

$$\beta_{ijk} \propto \frac{\partial \alpha_{ij}}{\partial q} \frac{\partial \mu_k}{\partial q} \quad (i, j, k = a, b, c), \quad [7]$$

where α_{ij} and μ_k are the polarizability and dipole moment, respectively, and q is the normal mode coordinate. By analyzing

the polarizability and dipole moment derivatives, we can deduce the values of β_{ijk} . According to group theory, only $\partial\mu_c/\partial q$ and $\partial\alpha_{ab}/\partial q = \partial\alpha_{ba}/\partial q$ are not equal to zero for the B_1 mode. Therefore, the nonzero hyperpolarizability tensor elements for the B_1 mode are $\beta_{abc} = \beta_{bac}$. Similarly, for the B_2 mode we have $\beta_{acb} = \beta_{cab}$, and for the B_3 mode we have $\beta_{bca} = \beta_{cba}$. Because SFG measurements are based on the surface or interface fixed coordinate system, it is necessary to transform observables from the molecular fixed axes (a, b, c) to the surface/interface fixed axes (x, y, z). Euler angles (χ, θ, ϕ) are used here to specify the orientation of the (abc) system with respect to the (xyz) system as depicted in ref. 76.

By assuming that the adsorbed peptide film is azimuthally symmetric, we have the following nonzero susceptibility tensor elements for the different modes (75, 76) as follows: B_1 mode,

$$\begin{aligned}\chi_{xxz} &= \chi_{yyz} = \chi_{zxx} = \chi_{zyz} = \chi_{zxx} = \chi_{zyy} \\ &= -N_s(\langle \cos\theta \sin\phi \cos\phi \rangle - \langle \cos^3\theta \sin\phi \cos\phi \rangle)\beta_{abc}\end{aligned}\quad [8a]$$

$$\chi_{zzz} = 2N_s(\langle \cos\theta \sin\phi \cos\phi \rangle - \langle \cos^3\theta \sin\phi \cos\phi \rangle)\beta_{abc}\quad [8b]$$

$$\begin{aligned}\chi_{xxy} &= -\chi_{zyx} = -\chi_{yxz} = \chi_{xzy} \\ &= \frac{1}{2}N_s(\langle \sin^2\theta \cos^2\phi \rangle - \langle \sin^2\theta \sin^2\phi \rangle)\beta_{abc};\end{aligned}\quad [8c]$$

B_2 mode,

$$\begin{aligned}\chi_{xxy} &= -\chi_{zyx} = -\chi_{yxz} = \chi_{xzy} \\ &= \frac{1}{2}N_s(\langle \cos^2\theta \rangle - \langle \sin^2\theta \cos^2\phi \rangle)\beta_{acb};\end{aligned}\quad [9]$$

and B_3 mode,

$$\begin{aligned}\chi_{xzy} &= -\chi_{zyx} = -\chi_{yxz} = \chi_{xzy} \\ &= -\frac{1}{2}N_s(\langle \cos^2\theta \rangle - \langle \sin^2\theta \sin^2\phi \rangle)\beta_{bca},\end{aligned}\quad [10]$$

where N_s is the surface density of the repeating unit of the β -sheet.

The achiral susceptibility tensor elements for the B_2 and B_3 modes have the same form as the B_1 mode except that β_{abc} should be replaced by β_{acb} and β_{bca} , respectively. Our SFG studies presented here (especially for the B_1 mode) confirm the recent suggestion that macromolecular orientational effects can dominate the chiroptical responses of uniaxial systems. Theoretical studies show that molecules with C_2 symmetry and asymmetric twist angles can generate strong chiral signals at interfaces (36). Here, Eqs. 9 and 10 indicate that even with random twist angle ϕ , molecules with D_2 symmetry may generate chiral signals (from the B_2 and B_3 modes).

According to Eqs. 8–10, if we assume that the twist angle ϕ has a random distribution, SFG signals from antiparallel β -sheets will be zero in normal (achiral) SFG spectra. The detection of SFG signals from antiparallel β -sheets in ssp and ppp spectra indicates that the twist angle ϕ does not have a random distribution. This characteristic is different from most small chemical groups, such as methyl and methylene groups, which usually have random twist angles at interfaces. Assuming δ

distributions for both θ and ϕ , we found that neither θ nor ϕ can be $0^\circ, 90^\circ, 180^\circ$, or 270° . Our results suggest that the antiparallel β -sheets of tachyplesin I are ordered at the PS/solution interface, and very likely they tilt at the interface, instead of being parallel or perpendicular to the PS surface normal.

Our spectral fitting results show that three peaks in the SFG spectra collected from interfacial tachyplesin I can be assigned to antiparallel β -sheets. The peak at $1,633\text{ cm}^{-1}$ belongs to the B_2 mode, and the peaks at $1,685$ and $1,695\text{ cm}^{-1}$ belong to the B_1 and B_3 modes. Further assignment (e.g., whether the $1,685\text{ cm}^{-1}$ peak is B_1 or B_3 mode) is difficult and should be discussed in the future. Theoretically, if we know such peak assignments, we can evaluate the detailed orientation of antiparallel β -sheets at interfaces based on Eqs. 8–10. For example, assuming that both θ and ϕ have δ distributions, we can calculate the magnitude of second-order nonlinear susceptibility tensor elements as a function of θ and ϕ according to Eqs. 8–10. As an example for such calculations, we show the dependence of χ_{yyz} of the B_1 mode on θ and ϕ in Fig. 5, which is published as supporting information on the PNAS web site. If all relative and/or absolute intensities of these three vibrational modes can be precisely measured by SFG spectra collected by using different polarization combinations of input and output beams, orientation information of tachyplesin I at the interface can be deduced from a comparison between the experimental data and such calculated curves. Further, more complicated relations between the magnitudes of second-order nonlinear susceptibility tensor elements and orientation angles θ and ϕ and their distributions without the assumption that they have to be δ distributions can be calculated. Then, by comparison between such relations and experimental data, average orientations of θ and ϕ and their distributions can be deduced. We believe that such detailed data analysis and orientation determination is feasible and will be reported in the future.

In the literature, SFG studies mostly focus on small chemical groups, such as methyl groups. Because of the symmetry of such “small” groups, the orientational measurements by SFG are often limited to the detection and analysis of $\langle \cos\theta \rangle$ and $\langle \cos^3\theta \rangle$. Our study of antiparallel β -sheets here shows that SFG can provide more orientational information about protein secondary structure at the interface, not only the θ angle distribution information, but also the twist angle (ϕ) distribution information. Our research presented in this work proves that antiparallel β -sheets can generate both chiral and achiral SFG signals, and perhaps more detailed structural information of interfacial β -sheets can be deduced from such SFG spectra.

Conclusion

In this work, we showed that it is possible to detect weak chiral SFG vibrational spectra from adsorbed protein in the amide I range at the solid/liquid interface by using an interference enhancement method. We also observed very strong chiral SFG vibrational spectra from a β -sheet peptide at the interface directly. Our results confirm the recent suggestion that macromolecular orientational effects can dominate the chiroptical responses of uniaxial systems. This finding indicates that besides the orientational information provided by normal SFG spectra, SFG can provide more secondary structural information of interfacial proteins from chiral spectra, demonstrating the potential to develop SFG into a powerful and unique technique to study protein and peptide structures at interfaces.

We thank Prof. Y. R. Shen for his advice and suggestions on this research. This work was supported by the National Science Foundation, Office of Naval Research, and University of Michigan.

1. Petralli-Mallow, T., Wong, T. M., Byers, J. D., Yee, H. I. & Hicks, J. M. (1993) *J. Phys. Chem.* **97**, 1383–1388.
2. Byers, J. D. & Hicks, J. M. (1994) *Chem. Phys. Lett.* **231**, 216–224.

3. Byers, J. D., Yee, H. I., Petralli-Mallow, T. & Hicks, J. M. (1994) *Phys. Rev. B Condens. Matter* **49**, 14643–14647.
4. Byers, J. D., Yee, H. I. & Hicks, J. M. (1994) *J. Chem. Phys.* **101**, 6233–6241.

5. Kauranen, M., Verbiest, T., Maki, J. J. & Persoons, A. (1994) *J. Chem. Phys.* **101**, 8193–8199.
6. Maki, J. J., Kauranen, M. & Persoons, A. (1995) *Phys. Rev. B Condens. Matter* **51**, 1425–1434.
7. Verbiest, T., Kauranen, M., Persoons, A., Ilkonen, M., Kurkela, J. & Lemmettyinen, H. (1994) *J. Am. Chem. Soc.* **116**, 9203–9205.
8. Verbiest, T., Kauranen, M. & Persoons, A. (1999) *J. Mater. Chem.* **9**, 2005–2012.
9. Verbiest, T., Elshocht, S. V., Kauranen, M., Hellemans, L., Snauwaert, J., Nuckolls, C., Katz, T. J. & Persoons, A. (1998) *Science*, **282**, 913–915.
10. Belkin, M. A., Kulakov, T. A., Ernst, K. H., Yan, L. & Shen, Y. R. (2000) *Phys. Rev. Lett.* **85**, 4474–4477.
11. Belkin, M. A., Han, S. H., Wei, X. & Shen, Y. R. (2001) *Phys. Rev. Lett.* **87**, 113001.
12. Han, S. H., Ji, N., Belkin, M. A. & Shen, Y. R. (2002) *Phys. Rev. B Condens. Matter* **66**, 16541.
13. Belkin, M. A. & Shen, Y. R. (2003) *Phys. Rev. Lett.* **91**, 213907.
14. Ji, N. & Shen, Y. R. (2004) *J. Am. Chem. Soc.* **126**, 15008–15009.
15. Hayashi, M., Lin, S. H. & Shen, Y. R. (2004) *J. Phys. Chem. A* **108**, 8058–8076.
16. Belkin, M. A., Shen, Y. R. & Flytzanis, C. (2002) *Chem. Phys. Lett.* **363**, 479–485.
17. Belkin, M. A., Kulakov, T. A., Ernst, K. H., Han, S. H. & Shen, Y. R. (2002) *Opt. Mater.* **21**, 1–5.
18. Belkin, M. A., Shen, Y. R. & Harris, R. A. (2004) *J. Chem. Phys.* **120**, 10118–10126.
19. Han, S. H., Belkin, M. A. & Shen, Y. R. (2004) *Opt. Lett.* **29**, 1527–1529.
20. Fischer, P., Wiersma, D. S., Righini, R., Champagne, B. & Buckingham, A. D. (2000) *Phys. Rev. Lett.* **85**, 4253–4256.
21. Fischer, P. & Buckingham, A. D. (1998) *J. Opt. Soc. Am. B* **15**, 2951–2957.
22. Champagne, B., Fischer, P. & Buckingham, A. D. (2000) *Chem. Phys. Lett.* **331**, 83–88.
23. Fischer, P., Buckingham, A. D. & Albrecht, A. C. (2001) *Phys. Rev. A At. Mol. Opt. Phys.* **64**, 053816.
24. Fischer, P., Beckwitt, K., Wise, F. W. & Albrecht, A. C. (2002) *Chem. Phys. Lett.* **352**, 463–468.
25. Yang, P. K. & Huang, J. Y. (1998) *J. Opt. Soc. Am. B* **15**, 1698–1706.
26. Schanne-Klein, M. C., Boulesteix, T., Hache, F., Alexandre, M., Lemereier, G. & Andraud, C. (2002) *Chem. Phys. Lett.* **362**, 103–108.
27. Hache, F., Mesnil, H. & Schanne-Klein, M. C. (2001) *J. Chem. Phys.* **115**, 6707–6715.
28. Petralli-Mallow, T., Plant, A. L., Lewis, M. L. & Hicks, J. M. (2000) *Langmuir* **16**, 5960–5966.
29. Hicks, J. M. & Petralli-Mallow, T. (1999) *Appl. Phys. B* **68**, 589–593.
30. Andrews, D. L. & Hands, I. D. (1998) *J. Phys. B At. Mol. Opt. Phys.* **31**, 2809–2824.
31. Hecht, L. & Barron, L. D. (1996) *Mol. Phys.* **89**, 61–80.
32. Zhang, Y. D., Li, J. Q. & Li, C. F. (2002) *Chin. Phys. Lett.* **19**, 791–794.
33. Simpson, G. J. (2002) *J. Chem. Phys.* **117**, 3398–3410.
34. Simpson, G. J., Perry, J. M. & Ashmore-Good, C. L. (2002) *Phys. Rev. B Condens. Matter* **66**, 165437.
35. Burke, B. J., Moad, A. J., Polizzi, M. A. & Simpson, G. J. (2003) *J. Am. Chem. Soc.* **125**, 9111–9115.
36. Simpson, G. J. (2004) *ChemPhysChem* **5**, 1301–1310.
37. Polizzi, M. A., Plocinik, R. M. & Simpson, G. J. (2004) *J. Am. Chem. Soc.* **126**, 5001–5007.
38. Conboy, J. C. & Kriech, M. A. (2003) *Anal. Chim. Acta* **96**, 143–153.
39. Wang, J., Even, M. A., Chen, X., Schmaier, A. H., Waite, J. H. & Chen, Z. (2003) *J. Am. Chem. Soc.* **125**, 9914–9915.
40. Shen, Y. R. (1984) *The Principles of Nonlinear Optics* (Wiley, New York).
41. Gragson, D. E. & Richmond, G. L. (1998) *J. Phys. Chem. B* **102**, 3847–3861.
42. Chen, Z., Shen, Y. R. & Somorjai, G. A. (2002) *Annu. Rev. Phys. Chem.* **53**, 437–465.
43. Bain, C. D. (1995) *J. Chem. Soc. Faraday Trans.* **91**, 1281–1296.
44. Kim, G., Gurau, M., Kim, J. & Cremer, P. S. (2002) *Langmuir* **18**, 2807–2811.
45. Gautam K. S. & Dhinojwala, A. (2002) *Phys. Rev. Lett.* **88**, 145501.
46. Richter, L. J., Yang, C. S.-C., Wilson, P. T., Hacker, C. A., van Zee, R. D., Stapleton, J. J., Allara, D. L., Yao, Y. & Tour, J. M. (2004) *J. Phys. Chem. B* **108**, 12547–12559.
47. Dreesen, L., Humbert, C., Sartenaer, Y., Caudano, Y., Volcke, C., Mani, A. A., Peremans, A., Thiry, P. A., Hanique, S. & Frere, J.-M. (2004) *Langmuir* **20**, 7201–7207.
48. McGall, S. J., Davies, P. B. & Neivandt, D. J. (2004) *J. Phys. Chem. B* **108**, 16030–16039.
49. Ye, S., Noda, H., Nishida, T., Morita, S. & Osawa, M. (2004) *Langmuir* **20**, 357–365.
50. Shen, Y. R. (1994) in *Proceedings of the International School of Physics “Enrico Fermi” Course CXX: Frontiers in Laser Spectroscopy*, eds. Hansch, T. W. & Inguscio, M. (North-Holland, Amsterdam), p. 139.
51. Dick, B., Gierulski, A. & Marowsky, G. (1985) *Appl. Phys. B* **38**, 107–116.
52. Higgins, D. A., Byerly, S. K., Abrams, M. B. & Corn, R. M. (1991) *J. Phys. Chem.* **95**, 6984–6990.
53. Simpson, G. J., Westerbuhr, S. G. & Rowlen, K. L. (2000) *Anal. Chem.* **72**, 887–898.
54. Wei, X., Hong, S. C., Zhuang, X. W., Goto, T. & Shen, Y. R. (2000) *Phys. Rev. E Stat. Phys. Plasmas Fluids Relat. Interdiscip. Top.* **62**, 5160–5172.
55. Wang, J., Chen, C. Y., Buch, S. M. & Chen, Z. (2001) *J. Phys. Chem. B* **105**, 12118–12125.
56. Wang, J., Clarke, M. L. & Chen, Z. (2004) *Anal. Chem.* **76**, 2159–2167.
57. Jung, S.-Y., Lim, S.-M., Albertorio, F., Kim, G., Gurau, M. C., Yang, R. D., Holden, M. A. & Cremer, P. S. (2003) *J. Am. Chem. Soc.* **125**, 12782–12786.
58. Peppas, N. A. & Langer, R. (1994) *Science*, **263**, 1715–1720.
59. Hubbell, J. A. (1995) *Biotechnology*, **13**, 565–576.
60. Anderson, J. M. (2001) *Ann. Rev. Mater. Res.* **31**, 81–110.
61. Babensee, J. E., Anderson, J. M., McIntire, L. V. & Mikos, A. G. (1998) *Adv. Drug Delivery Rev.* **33**, 111–139.
62. Zhuang, X., Miranda, P. B., Kim, D. & Shen, Y. R. (1999) *Phys. Rev. B Condens. Matter* **59**, 12632–12640.
63. Bertie, J. E., Ahmed, M. K. & Eysel, H. H. (1989) *J. Phys. Chem.* **93**, 2210–2218.
64. Picard, F., Buffeteau, T., Desbat, B., Auger, M. & Pérolet, M. (1999) *Biophys. J.* **76**, 539–551.
65. Hancer, M., Sperline, R. P. & Miller, J. D. (2000) *Appl. Spectrosc.* **54**, 138–143.
66. Barth, A. & Zscherp, C. (2002) *Q. Rev. Biophys.* **35**, 369–430.
67. Hilario, J., Kubelka, J. & Keiderling, T. A. (2003) *J. Am. Chem. Soc.* **125**, 7562–7574.
68. Moore, W. H. & Krimm, S. (1975) *Proc. Natl. Acad. Sci. USA* **72**, 4933–4935.
69. Tatulian, S. A. & Tamm, L. K. (1997) *Q. Rev. Biophys.* **30**, 365–429.
70. Laederach, A., Andreotti, A. H. & Fulton, D. B. (2002) *Biochemistry* **41**, 12359–12368.
71. Chen, X. Y., Wang, J., Sniadecki, J. J., Even, M. A. & Chen, Z. (2005) *Langmuir*, in press.
72. Li, Y.-J., Rothwarf, D. M. & Scheraga, H. A. (1998) *J. Am. Chem. Soc.* **120**, 2668–2669.
73. Krimm, S. & Bandekar, J. (1986) *Adv. Prot. Chem.* **38**, 181–367.
74. Duffy, D. C., Davies, P. B. & Bain, C. D. (1995) *J. Phys. Chem.* **99**, 15241–15246.
75. Moad, A. J. & Simpson, G. J. (2004) *J. Phys. Chem. B* **108**, 3548–3562.
76. Hirose, C., Akamatsu, N. & Doman, K. (1992) *Appl. Spectrosc.* **46**, 1051–1071.